IEEE Access
Multidisciplinary | Rapid Review | Open Access Journal

Received 12 March 2024, accepted 20 May 2024, date of publication 24 May 2024, date of current version 3 June 2024.

Digital Object Identifier 10.1109/ACCESS.2024.3405192

RESEARCH ARTICLE

Deep Learning Multi-User Detection for PD-SCMA

SIMON CHEGE, (Member, IEEE), AND TOM WALINGO, (Member, IEEE)
Discipline of Electrical, Electronic and Computer Engineering, University of KwaZulu-Natal, Durban 4000, South Africa
Corresponding author: Simon Chege (schegemathinji@gmail.com)

ABSTRACT The performance of hybrid multi-radio access technologies depends on the sufficiency of the multi-user detection (MUD) at the receiver. For optimal performance of the hybrid power-domain sparse code multiple access (PD-SCMA), robust detection strategies are necessary to alleviate MUD complexity and reduces computational time. Deep learning (DL) based MUD techniques are the most promising as they can detect all symbols of an overloaded PD-SCMA without requiring additional operations of channel estimation and interference cancellation. This work proposes a deep neural network (DNN) aided MUD scheme (DNN-MUD) for an uplink PD-SCMA system supporting near users (NUs) and far users (FUs) multiplexed in power-, and code-domain, respectively. The proposed DNN-MUD features a unified framework that jointly performs successive interference cancellation (SIC) and message passing algorithm (MPA)/expectation propagation algorithm (EPA) operations to overcome interference propagation of SIC and computational complexity of MPA/EPA. The DNN training is enhanced by batch normalization to reduce the internal covariant shifts, thus enhancing the efficiency of detection. Performance results show that the average symbol error rate (SER), complexity and computational time of the proposed DNN-MUD significantly outperforms the conventional joint SIC-MPA/EPA schemes.

INDEX TERMS PD-SCMA, deep learning, multi-user detection, batch normalization, SER.

I. INTRODUCTION

Amongst the key enablers of beyond 5G (B5G) networks, hybrid multi-radio access technologies are fundamental players in satisfying the ubiquitous quality of service (QoS) demands of the ever explosively growing number of wireless devices. Non-orthogonal multiple access (NOMA) is a powerful transmission technique developed to enhance spectral efficiency compared to orthogonal multiple access (OMA) schemes [1]. Besides, hybrid NOMA allows overloading and massive connectivity by multiplexing in both power (PD) and code domains (CD) at the expense of increased receiver complexity. In particular, at the transmitter, power domain sparse code multiple access (PD-SCMA) enhances capacity by co-multiplexing near users equipments (NUs) and far user equipments (FUs) using PD-NOMA into a codebook by allocation of distinct power levels, while exclusively assigning codes to the NU-FU clusters. At the receiver, a joint multi-user detection (MUD) featuring successive interference cancellation (SIC) and message passing algorithm (MPA) is deployed to iteratively decode the user symbols [2], [3], [4], [5].

In PD- NOMA, the application of deep learning (DL) techniques for SIC is gaining traction due to the practical limitation of SIC resulting from lack of perfect channel state information (CSI) statistics and error propagation due to cumulative interference. The belief propagation and expectation propagation based detection schemes deploying maximum likelihood exhibit high computational complexity [6]. A hybrid deep neural network (HyDNN) - SIC model for multi-user uplink channel estimation (CE) and signal detection (SD) is proposed in [7] to optimize system loss. To optimise SIC, an intelligent SIC sorting and detection scheme (I-SIC) that learns the implied characteristics in the received signal, channel state information (CSI) and power information via DL is proposed in [8]. In [9], a convolutional neural network (CNN) based SIC is proposed to solve SIC imperfections and mitigate losses therein, hence improving the sum rate of the decoded signal. In MIMO-NOMA, a deep neural network (DNN) aided SIC is proposed in [10] to jointly optimize the precoder and SIC decoding by minimizing the mean square error (MSE) at

The associate editor coordinating the review of this manuscript and approving it for publication was Ghufran Ahmed.

each step. Although it outperforms the conventional SIC, the proposed DNN-SIC at each step suffers high computational complexity. Further, such a scheme is deployed for MIMO-NOMA in [11]. A DL-SIC scheme for Faster-than-Nyquist (FTN) modulated NOMA utilizing the sliding window detection is proposed [12]. Generally, DL techniques are applied in PD-NOMA due to their faster computational time, easily configurable, more consistent and reliable performance indices [13]. Furthermore, DL can significantly reduce the computational complexity at the training and testing stages of encoding, resource management and decoding [14]. Additionally, DL can potentially provide significant system-level improvements as compared to the conventional model-based approach for solving highly dimensional, non-convex optimization problems [15]. Therefore, this work intents to harvest the advantages of DL techniques by extending them to the PD-NOMA access scheme.

For the SCMA, DL has demonstrated great competence in enhancing the bit error rate (BER) performance compared to generic decoding algorithms [16]. The work in [17] unfolds the MPA procedure and converts it to a sparsely connected NN treating the weights as the parameters of the NN. A DL SCMA decoder trained based on the mean square error (MSE) loss function is proposed in [18] and [19]. Authors in [20] regard the decoding strategy as a non-mutually exclusive classification problem and deploy the sigmoid function in the decoder's output layer as the activation function. Differently, [21] flips the SCMA decoding strategy as a multi-output classification problem, rather than a single-output classification problem. This flip eases the NN training, consequently, achieving a better BER performance with reduced computational complexity. A jointly designed and trained denoising auto-encoder (DAE) and DNN for SCMA signals decoding over an additive white Gaussian noise (AWGN) channel is proposed in [22]. The proposed DAE-DNN detection strategy outperforms the previously modelled DL schemes albeit exhibiting under-performance compared to the conventional MPA. Unlike MPA, the DAE-DNN detector assumes unavailability of SCMA codebook knowledge at the receiver end, making the comparison unfair. In contrast, the application of DL in SCMA results in assumes codebook knowledge availability is proposed, providing a fair comparison to the MPA and indeed presenting a better BER performance than MPA.

Generic MUD's have been applied on hybrid NOMA [2], [3], [4], [5], [23], [24]. Although there has been significant effort to improve signal detection and reconstruction strategies at reception, generic algorithms still exhibit sub-optimality. Besides, with increased resource overloading, generic algorithms saturate thereby limiting the multiplexing potential of a hybrid NOMA scheme. In addition, the generic MUDs based architectures exhibit error propagation, increased computational complexity and longer computational time as the number of user equipment's in the system bulge. Significant research on DL aided detection is carried out for SCMA and PD-NOMA detection independently, and only a few works have focused on DL deployment for hybrid NOMA. The blends of MUDs for hybrid NOMA detection that combine PD-NOMA's parallel interference cancellation (PIC) and SIC with SCMA's expectation propagation algorithm (EPA) and MPA are still devoid of a unified signal processing framework. By using DL to improve the MUD, a more unified architecture exhibiting better SER, shorter computation times and reduced complexity is realizable [25]. In [26], an uplink hybrid NOMA scheme (HMAS) that jointly adopts OFDMA and SCMA to support NUs and FUs respectively is developed. The proposed detector significantly outperforms the conventional joint MPA-SIC detector. In [27], a hybrid NOMA (HNOMA) is proposed using both PD and CD NOMA for multiple access of grouped users. A DNN-based demodulator trained offline then deployed online is proposed in [28] to recover transmitted bit streams for PDSCMA- VLC. Given the potential performance associated with DL aided detection schemes in PD-NOMA, SCMA and hybrid NOMA, this work considers the deployment of DL based decoding model for the multidimensional new hybrid PD-SCMA NOMA scheme.

The PD-SCMA scheme exhibits significant potential in enhancing capacity and allowing overloading of the spectral resources [3], [5]. However, the complexity of the SIC-MPA based detection, increased signal distortions and the need for higher signal to noise ratio (SNR) to counter the bulging interference in both domains as the number of layers and codebooks increase, necessitates a paradigm shift in the MUD technology. To the best of our knowledge, the full potential of a unified DL aided architecture for a hybrid NOMA detection performance has not yet been exploited. This work proposes a deep neural network aided MUD scheme (DNN-MUD) for an uplink PD-SCMA system featuring;

- A network model where Near users (NUs) and far users (FUs) are multiplexed in power-, and code - domain, respectively.
- A unified DL-MUD architecture utilizing a deep neural network (DNN) model that jointly performs the SIC and MPA, and overcome the limitations of the conventional MUDs. Unlike the works of [26] and [28], the DNN-MUD features a fully connected structure utilizing stochastic gradient descent for iterative updates of weights and biases via back-propagation.
- A DNN training enhanced by batch normalization to reduce the internal covariant shifts. Unlike in [28], the training learning rate is increased, thus enhancing the efficiency of detection.
- Performance results illustrating that the average symbol error rate (SER), computational time and complexity of the proposed DL-MUD significantly outperforms the joint SIC-EPA schemes.

II. SYSTEM MODEL

A. UPLINK PD-SCMA SYSTEM

The uplink PD-SCMA transceiver model illustrated in FIGURE 1 supports sets of $\mathcal{J}$ NUs and $\mathcal{K}$ FUs operating

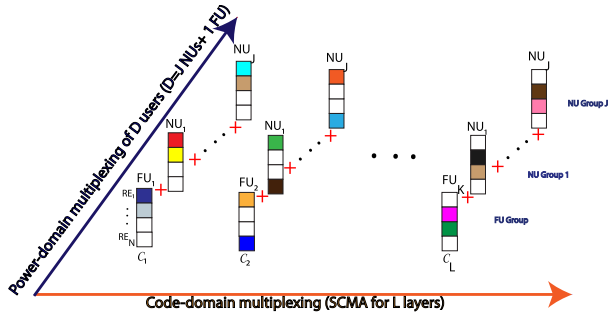

FIGURE 1. PD-SCMA block with $D = J + 1$, $J \in J_{CB}$ superimposed NUs, $L = K$ layers/codebooks and $N = 4$ REs.

$L = K$ layers (of set $\mathcal{L}$) and N orthogonal resource elements (REs), with $N \ll L$. Each layer spreads its data over d_v, ($d_v < N$) REs. A layer is constructed by drawing select codewords from each user equipment (UE) of FU set $\mathcal{K}$, $|\mathcal{K}| = K$ and clustered NU set $\mathcal{J}_{CB}$, ($|\mathcal{J}_{CB}| = J$, $\mathcal{J}_{CB} \in \mathcal{J}$). This implies that a layer constitutes $D = (J + 1)$ users symbols. Under the constraint that no two layers should be assigned all the same resource units (RUs) for an affordable complexity order, a system is fully loaded if $\lambda = D \times \binom{L}{d_v}$, where λ denotes the overloading factor.

At the PD-SCMA transmitter, $J-$NUs ($K-$FUs) map $Q-$ary modulated symbols $b^{\mathcal{J}}(b^{\mathcal{K}}) = \{b_j^{\mathcal{J}}\}_{j=1}^{J}(\{b_k^{\mathcal{K}}\}_{k=1}^{K})$ into $\{\mathbf{x}_j^{\mathcal{J}}\}_{j=1}^{J}(\{\mathbf{x}_k^{\mathcal{K}}\}_{k=1}^{K})$, where the column vectors $\mathbf{x}_j^{\mathcal{J}}(\mathbf{x}_k^{\mathcal{K}}) = \{x_{jn}^{\mathcal{J}}\}_{n=1}^{N\times 1}(\{x_{kn}^{\mathcal{K}}\}_{n=1}^{N\times 1}) \in \mathbb{C}^N \in \mathcal{X}_{j(k)}$ is the $N-$dimensional sparse codeword with $K - N$ zeros and transmit them over the $N-$resource elements. Denote by $a_{k,j}$ the pairing policy. While in SCMA, a constraint $\sum_{j\in\mathcal{J}} a_{k,j} \leq 1, \forall k$ holds true, that is, a codebook can be assigned to at most one user equipment, in PD-SCMA, $\sum_{j\in\mathcal{J}} a_{k,j} \leq J, \forall k$ allows pairing upto J users with distinct power levels.

At the receiver, the received signal vector $\mathbf{r}$ is given by

$$\mathbf{r} = \sum_{k=1}^{K} \sqrt{P^{\mathcal{K}}}\,\mathrm{diag}(\mathbf{h}_k^{\mathcal{K}})\mathbf{x}_k^{\mathcal{K}} + \sum_{k=1}^{K}\sum_{j=1}^{J} \sqrt{P^{\mathcal{J}}}\,\mathrm{diag}(\mathbf{h}_j^{\mathcal{K}})\mathbf{x}_j^{\mathcal{J}} + \mathbf{v}, \tag{1}$$

where $P^{\mathcal{J}}$ and $P^{\mathcal{K}}$ denote the NUs and FUs transmission powers. $\mathbf{h}_j^{\mathcal{K}}(\mathbf{h}_k^{\mathcal{K}}) = \{h_{j,n}^{\mathcal{K}}\}_{n=1}^{N}(\{h_{k,n}^{\mathcal{K}}\}_{n=1}^{N}) \in \mathbb{C}^{1\times N}$ denote the channel gain vectors from the $j^{th}(k^{th})$ NU (FU) to the receiver. It is assumed that $\|\mathbf{h}_j^{\mathcal{K}}\| \gg \|\mathbf{h}_k^{\mathcal{K}}\|, \forall j, k$. $\mathbf{v} \sim \mathcal{CN}(0, N_0\mathbf{I}_N)$ represents additive white Gaussian noise (AWGN) vector.

B. JOINT EPA-SIC BASED PD-SCMA DETECTION

The received signal over the PD-SCMA block given by (1) is iteratively decoded through EPA and SIC. EPA is selected over MPA for the code-domain decoding since it exhibits a lower complexity [5]. Firstly, the EPA decodes all the user signals that are superimposed in the codebooks $\hat{\mathbf{r}}_{CB}$, based on a factor graph. Secondly SIC is deployed to obtain the power distinct NU and FU groups, then lastly, after signal reconstruction and cancellation, MPA is deployed to decode

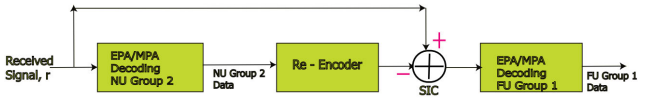

FIGURE 2. PD-SCMA EPA-SIC detection for two near and far user groups.

Algorithm 1 Joint EPA-SIC Detection

Input: $\mathbf{h}^{\mathcal{J}}$, $\mathbf{h}^{\mathcal{K}}$, $P^{\mathcal{J}}$, $P^{\mathcal{K}}$, J, K, N.
Initialization: Iteration number, τ
Average $P^{\mathcal{J}}|\mathbf{h}^{\mathcal{K}}|^2$, $P^{\mathcal{K}}|\mathbf{h}^{\mathcal{K}}|^2$.
Apply EPA $\mathbf{r}$ eqn. (1).
Output: $\hat{\mathbf{r}}_{\mathbf{CB}}$.
Apply SIC on $\hat{\mathbf{r}}_{\mathbf{CB}}$.
Output: $\hat{\mathbf{r}}_{\mathbf{CB}} = \hat{\mathbf{r}}_{\mathbf{CB}} - \sum_{j\in\mathcal{J}} \sqrt{P^{\mathcal{J}}}\,\mathrm{diag}(\mathbf{h}_j^{\mathcal{J}})\mathbf{x}_j^{\mathcal{J}}$.
if $\tau = D$ **then**
  Employ EPA on $\mathbf{r}$ to obtain user-specific symbols.
else
  Set $\tau = \tau + 1$
  Set $P^{\mathcal{J}}|\mathbf{h}^{\mathcal{J}}|^2 = P^{\mathcal{J}}|\mathbf{h}^{\mathcal{J}}|^2 - P_\tau|h_\tau|^2$
end if
Go back to 4.

the user-specific symbols in each group as illustrated in Figure 2 for a simplified scenario of two near and far user groups. With SIC, a user detects the signals of all other users that are worse than itself according to the metric used and removes them from the received signal. This user treats the signal of all users better than itself as interference plus noise. Without loss of generality, it is assumed that users on different codebooks do not interfere with each other and only users with the same codebook produce interference over each other. Therefore by sorting users, we mean sorting users that are using the same codebook. The joint EPA-SIC iterative decoding process is summarised in Algorithm 1.

Based on the channel information and given that $P^{\mathcal{K}} \gg P^{\mathcal{J}}$ and, SIC treats (2) below as interference plus noise term and thus detects the FUs from $\mathbf{r}$ in (1).

$$\sum_{k=1}^{K}\sum_{j=1}^{J} \sqrt{P^{\mathcal{J}}}\,\mathrm{diag}(\mathbf{h}_j^{\mathcal{K}})\mathbf{x}_j^{\mathcal{J}} + \mathbf{v} \tag{2}$$

Consequently, the j^{th} NU detects the worse NUs ($i > j$) and removes them from the received signal while treating ($i < j$) NUs as noise. The resultant available signal $\hat{\mathbf{r}}$ is then given as

$$\hat{\mathbf{r}}_{\mathbf{CB}} = \sum_{k=1}^{K} \sqrt{P^{\mathcal{K}}}\,\mathrm{diag}(\mathbf{h}_k^{\mathcal{K}})\mathbf{x}_k^{\mathcal{K}} + \sum_{\substack{i\in\mathcal{J} \\ P_i^{\mathcal{J}} > P_j^{\mathcal{J}}}} \sqrt{P^{\mathcal{J}}}\,\mathrm{diag}(\mathbf{h}_i^{\mathcal{K}})\mathbf{x}_i^{\mathcal{J}} + \mathbf{v}. \tag{3}$$

After detecting all the J NUs, the resultant available signal at the receiver $\hat{\mathbf{r}}_{\mathbf{CB}}$ consist of the FUs signals and can be given by

$$\hat{\mathbf{r}}_{\mathbf{CB}} = \sum_{k=1}^{K} \sqrt{P^{\mathcal{K}}}\,\mathrm{diag}(\mathbf{h}_k^{\mathcal{K}})\mathbf{x}_k^{\mathcal{K}} + \mathbf{v}. \tag{4}$$

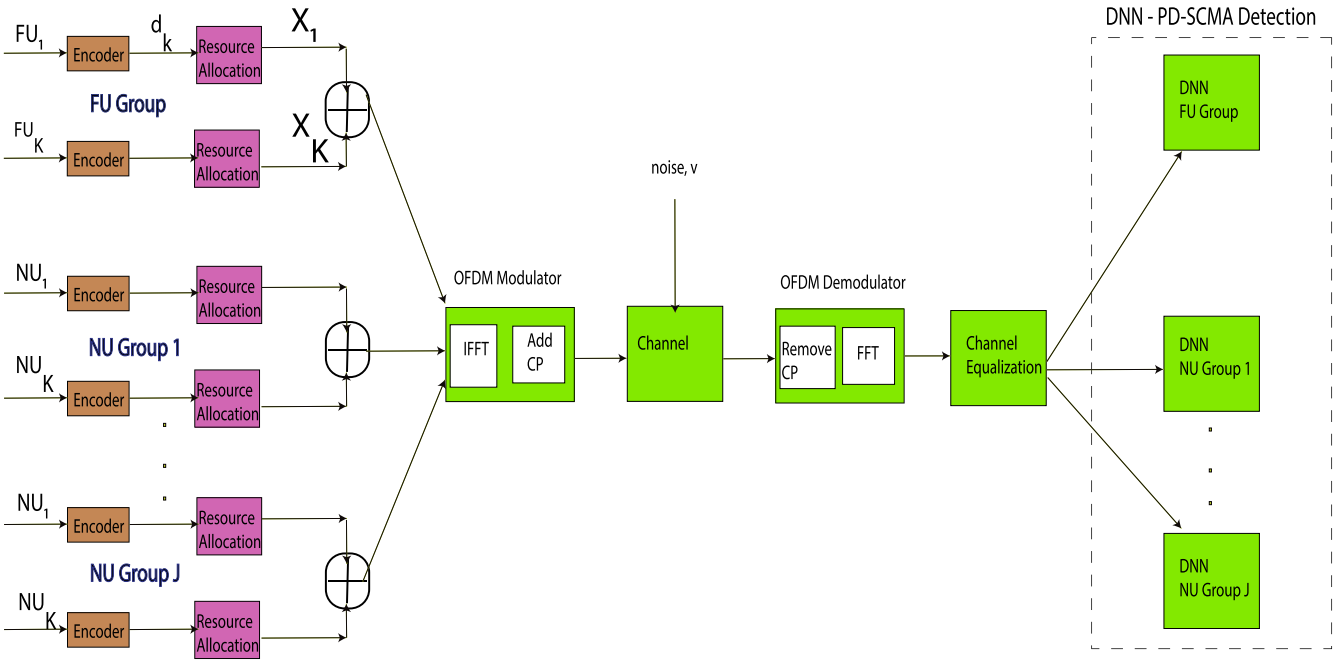

FIGURE 3. Block diagram for PD-SCMA system with a DNN.

The receiver complexity orders of PD-NOMA and SCMA are individually analysed in [29] and given as $\mathcal{O}((2D^3) + (2D^2)(C)(D-1))$ and $\mathcal{O}(I_T|M|^{d_v})$, respectively, where D denotes the number of user equipments (UEs) superimposed on a codebook, C is the number of codebooks assigned to a user, I_T denotes the total number of iterations, M is the codebook set size and d_v is the codebook sparsity degree. In PD-SCMA, each codebook is assigned to D UEs simultaneously, each UE performs EPA $D-$times and SIC $D-1$ times. Consequently, if a PD-SCMA utilizes C number of codebooks per UE, then the complexity order can be given by $\mathcal{O}(I_T|M|^{d_v}(C)(D))$.

III. PROPOSED DEEP LEARNING AIDED PD-SCMA DETECTION SCHEME

The block diagram of the PD-SCMA NOMA with the proposed DNN based MUD is given in FIGURE 3. At the transmitter, the NUs and FUs are first encoded, allocated resources and clustered into the SCMA blocks prior to being combined and applied to the inverse Fast Fourier transform (IFFT) module. The FUs and NUs in the same cluster i.e. in the same power-domain multiplexing level (PDML), are allocated the same power level. A cyclic prefix is added in front of each symbol and frame to combat inter-symbol interference (ISI) and then a preamble added for channel state information and synchronization. The symbols are then transmitted in a AWGN channel. At the receiver, frame synchronization is applied to the PD-SCMA received signal vector prior to applying to the channel equalizer. Frame synchronization identifies incoming frame/cluster alignment symbols while channel equalization tries to revert the many channel impairments thereby enhancing the MUD's detection capability.

From (1), we can write the recieved signal $\mathbf{r}$ given as

$$\mathbf{r} = \sqrt{P^{\mathcal{K}}}\mathbf{X}^{\mathcal{K}}\mathbf{H}^{\mathcal{K}} + \sum_{k=1}^{K}\sqrt{P^{\mathcal{J}}}\mathbf{X}^{\mathcal{J}}\mathbf{H}_k^{\mathcal{J}} + \mathbf{v}, \tag{5}$$

where $\mathbf{X}^{\mathcal{K}} = \sum_{k=1}^{K}\mathbf{x}_k^{\mathcal{K}}$, $\mathbf{X}^{\mathcal{J}} = \sum_{j=1}^{J}\mathbf{x}_j^{\mathcal{J}}$, $\mathbf{H}^{\mathcal{K}} = \text{diag}[h_1^{\mathcal{K}}h_2^{\mathcal{K}}\cdots h_N^{\mathcal{K}}]$ and $\mathbf{H}_k^{\mathcal{J}} = \text{diag}[h_{1k}^{\mathcal{J}}h_{2k}^{\mathcal{J}}\cdots h_{Nk}^{\mathcal{J}}]$. The NUs have higher channel gains compared to the FUs and therefore allocated lower power levels i.e., $\|\mathbf{h}_j^{\mathcal{J}}\| \gg \|\mathbf{h}_k^{\mathcal{K}}\|$ and therefore $\|\mathbf{P}^{\mathcal{K}}\| \gg \|\mathbf{P}^{\mathcal{J}}\|, \forall j,k$ and that $\|\mathbf{P}_1^{\mathcal{J}}\| > \|\mathbf{P}_2^{\mathcal{J}}\| > \cdots > \|\mathbf{P}_J^{\mathcal{J}}\|$. Given that power allocation and treating $\sum_{k=1}^{K}\sqrt{P^{\mathcal{J}}}\mathbf{X}^{\mathcal{J}}\mathbf{H}_k^{\mathcal{J}} + \mathbf{V}$ as the interference plus noise term, based on $\mathbf{r}$, the receiver will detect FUs data $\hat{\mathbf{f}}^{\mathcal{K}} = \{\hat{f}_k^{\mathcal{K}}\}_{k=1}^{K}$. The receiver then re-encodes the decoded data $\hat{\mathbf{f}}^{\mathcal{K}}$ to $\{\hat{\mathbf{x}}_k^{\mathcal{K}}\}_{k=1}^{K}$ and cancel it from $\mathbf{r}$ to yield

$$\hat{\mathbf{r}} = \sum_{k=1}^{K}\sqrt{P^{\mathcal{J}}}\mathbf{X}^{\mathcal{J}}\mathbf{H}_k^{\mathcal{J}} + \underbrace{\sqrt{P^{\mathcal{K}}}\mathbf{H}^{\mathcal{K}}(\mathbf{X}^{\mathcal{K}} - \hat{\mathbf{X}}^{\mathcal{K}}) + \mathbf{v}}_{Interference+Noise}. \tag{6}$$

As observed in subsection II-B, the joint EPA-SIC exhibits high computational complexity and is prone to SIC-induced error propagation. Using the proposed deep learning aided MUD, the data of the $D \times L$ users can be directly be decoded following frame synchronization and channel equalization. All the clusters and their clustered NUs and FUs use the same trained DNN to recover the transmitted bit streams.

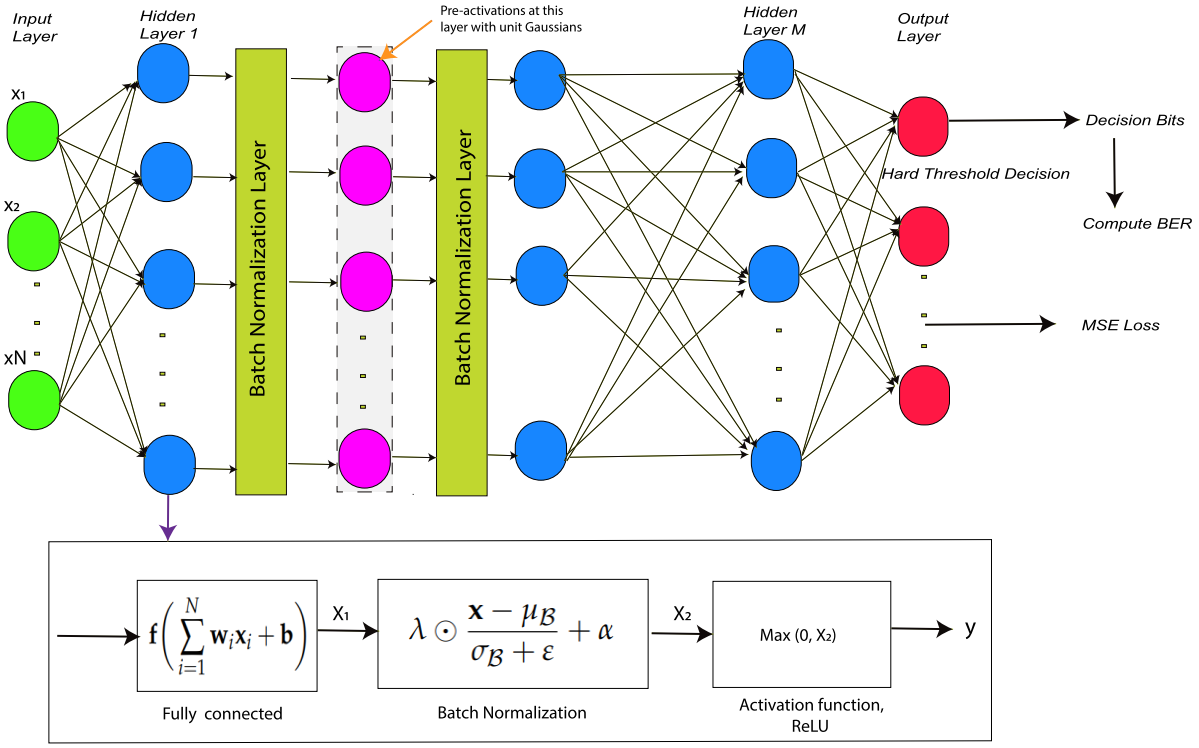

FIGURE 4. The network structure of the proposed DNN.

A. PROPOSED FULLY CONNECTED DNN STRUCTURE

The proposed DNN based MUD structure illustrated in FIGURE. 4 features a fully connected DNN comprising of an input layer with A_0 input neurons, M hidden layers with A_m neurons in each layer and an output layer with A_{M+1} output neurons. The DNN input layer are the data streams from the N resource elements. Denote by $\mathbf{W}_1$ the weight matrix $A_1 \times A_0$ containing the relationship between the input neurons and the first hidden layer neurons, $\mathbf{W}_m$ the weight matrix $A_{m+1} \times A_m$ between the hidden layer units and $\mathbf{W}_{M+1}$ the weight matrix $A_{M+1} \times A_M$ relation between the last hidden layer neurons and the output neurons. Likewise, the input biases, m^{th} hidden layer biases and output biases are stored respectively, in the $A_1 \times 1$, $A_m \times 1$ and $A_{M+1} \times 1$ bias vectors $\mathbf{b}_1$, $\mathbf{b}_{m+1}$ and $\mathbf{b}_{M+1}$. The input, hidden and output layer nodes are fully connected with each node at hidden and output layer being a computing unit given by,

$$\mathbf{y} = \mathbf{f}\left(\sum_{i=1}^{N} \mathbf{w}_i \mathbf{x}_i + \mathbf{b}\right) \tag{7}$$

where $\mathbf{y}$ and $\mathbf{x}_i$ are the output and the input of the i^{th} node, respectively, and $\mathbf{f}(\cdot)$ is the activation function that introduces a non-linearity which is important for the so-called expressive power of the DNN.

The DNN framework works as a functional estimator to map the input vector $\mathbf{s} = \mathbf{s}_0$ into the output vector $\hat{\mathbf{r}}$. In the proposed DNN-MUD structure, a leaky rectified linear unit (ReLU) activation function given by eqn. (9) is applied in the input layer and hidden layers. Starting from the input layer, the entries of $\mathbf{s}$ are fed to the first hidden layer and the neurons of the m^{th} hidden layer compute their activated values $\mathbf{s}_m$ as [30]

$$\mathbf{s}_m = ReLU(\mathbf{W}_m \mathbf{s}_{m-1} + \mathbf{b}_m), m = 1, 2, \cdots, M. \tag{8}$$

The $\mathbf{s}_m$ is then fed into the next hidden layer.

$$ReLU(s) = \begin{cases} s, & s \geq 0 \\ 0, & s < 0 \end{cases}. \tag{9}$$

At the output layer, the output mapping is given by

$$\hat{\mathbf{r}} = \chi(\mathbf{W}_{M+1} \mathbf{s}_M + \mathbf{b}_{M+1}). \tag{10}$$

Here, the output layer utilizes the Sigmoid function denoted as $\chi(\cdot)$ given by (11).

$$f_{sig}(s) = \frac{1}{1 + exp(-s)}. \tag{11}$$

The ReLU activation is employed since it saves and maps the features of the activated neurons besides mitigating gradient dispersion thereby solving the vanishing gradients issue. The ReLU function is computational cheaper as it requires only the $max(\cdot)$ function and easier to optimize even while implementing in a large DNN structure. Due to its piecewise linear functionality, ReLU will output the input directly if it is positive, otherwise, it will output zero, hence suitable for DNN's ease of training and improved performance.

B. DNN - MUD

In this proposed DNN-MUD structure, batch normalization (BN) is added for each node of the hidden layers. For every neuron (activation) in a particular layer, we can force the pre-activations to have zero mean and unit standard deviation. With BN, at each training iteration, this can be achieved by first subtracting the mean from each of the input features across the mini-batch and dividing by the standard deviation, where both are estimated based on the statistics of the current mini-batch. Secondly, a scale coefficient and an offset are applied to recover the lost degrees of freedom. Denoting by $\mathcal{B}$ a mini-batch and letting $\mathbf{x} \in \mathcal{B}$, be an input to batch normalization (BN).The batch normalization can be given as

$$BN(\mathbf{x}) = \lambda \odot \frac{\mathbf{x} - \mu_{\mathcal{B}}}{\sigma_{\mathcal{B}} + \varepsilon} + \alpha \tag{12}$$

where $\mu_{\mathcal{B}}$ and $\sigma_{\mathcal{B}}$ is the mean and standard deviation of the mini-batch $\mathcal{B}$ [20]. After applying standardization, the resulting mini-batch has zero mean and unit variance. The elementwise scale parameter λ and shift parameter α adopt the same shape as input $\mathbf{x}$ and are applied to recover the degree of freedom. The λ and α are learnable such that it's possible to go back from the normalized pre-activations to the actual distributions that the pre-activations follow. A small constant $\varepsilon > 0$ is added to the variance estimate $\sigma_{\mathcal{B}}$ to ensure that we never attempt division by zero, even in cases where the empirical variance estimate might be very small or vanishes.

1) TRAINING STAGE

At the training stage, the learning process is formalized as a minimization of the cost function. To train the proposed DL-MUD with the aim of optimizing the trade-off between the overall complexity and the link performance, stochastic gradient descent is selected to update the weights and biases iteratively via back-propagation as follows;

$$\theta_{\tau+1} = \theta_{\tau} - \eta \nabla_{\theta} \mathbf{J}(\theta), \tag{13}$$

where θ_{τ}, τ, η, ∇_{θ} and $\mathbf{J}(\theta)$ respectively denote the parameter (SER) to be optimized, the iteration number, the scalar-valued step size, the derivative with respect to θ and the MSE cost function expressed as

$$\mathbf{J}(\theta) \Rightarrow MSE = \frac{1}{D} \sum_{i=1}^{D} (\mathbf{r}_i - \hat{\mathbf{r}}_i)^2. \tag{14}$$

To ensure a fast training process, an approximation of the MSE criterion in (14) is computed by using random mini-batch training samples at each iteration τ, given by

$$\mathbf{J}_{\tau}(\theta) = \frac{1}{D_{\tau}} \sum_{i=1}^{D_{\tau}} \left(\mathbf{r}_{(\tau-1)D_{\tau}+i} - \hat{\mathbf{r}}_{(\tau-1)D_{\tau}+i} \right)^2. \tag{15}$$

with D_{τ} denoting the mini-batch size. Consequently, the training samples are split into $\mathcal{B} = \frac{D}{D_{\tau}}$ which are shuffled before every epoch, where each epoch has both one forward and one backward pass of all the training samples. In the training phase, the transmitted signal vectors $\mathbf{x}_k^{\mathcal{K}}$ and $\mathbf{x}_j^{\mathcal{J}}$, the channel gains $\mathbf{h}_k^{\mathcal{K}}$ and $\mathbf{h}_j^{\mathcal{K}}$ and the noise vector $\mathbf{V}$ are uniformly and independently drawn from the codebook as illustrated in subsection II-A.

2) DETECTION STAGE

The implementation of the detection phase is illustrated in Algorithm 2. The received signal vector $\mathbf{r}$ and the channel gain vectors $\mathbf{h}_k^{\mathcal{K}}$ and $\mathbf{h}_j^{\mathcal{K}}$ are utilized in computing the belief propagation and equivalent probabilities for EPA [31]. Consequently, these available data is employed as the input labels for the DNN to approximate the received signal. The decoding process is then performed using a low complexity iterative process same as one within the joint EPA-SIC proposed in Algorithm 1.

Algorithm 2 DNN Approaching Joint EPA-SIC Detection Algorithm

Input: $\mathbf{r}$, $\mathbf{h}_k^{\mathcal{K}}$ and $\mathbf{h}_j^{\mathcal{K}}$, $\mathbf{V}$, $\mathbf{W}_m$, $\mathbf{b}_m$
Output: *LLRs*
Initialization: Perform batch normalization.
for j=1:J, k=1:K, n=1:N and l=1:L **do**
  for $\mu = 1$ to training epoch **do**
    for $\psi = 1$ to num batch **do**
      Perform belief propagation and equivalent probabilities of EPA [31].
      Reconstruct the received signal $\mathbf{r}_n$ and the channel gains $\mathbf{h}_k^{\mathcal{K}}$ and $\mathbf{h}_j^{\mathcal{K}}$ into the form of DNN input vector.
      Perform SIC
      Obtain the approximated belief interval via the DNN
      for m=1:M **do**
        $\mathbf{s}_m = ReLU(\mathbf{W_m s} + \mathbf{b}_m)$
      end for
      $\hat{\mathbf{r}} = \chi(\mathbf{W}_{M+1}\mathbf{s}_M + \mathbf{b}_{M+1})$
      DNN training to approximate joint EPA-SIC by minimizing eq. (14) and eq. (15).
    end for
  end for
end for
DNN Data Testing: Normalizing outputs for at each iteration.
Log-Likelihood ratio (LLR) Computation same as the one in Algorithm 1.

C. COMPUTATIONAL COMPLEXITY ANALYSIS

The complexity analysis of EPA algorithm is primarily computed based on messages passing between the variable nodes (VNs) and the function nodes (FNs), plus the calculations of the posterior likelihood ratio after algorithm convergence. It can be observed that the complexity of EPA linearly scales both the codebook size Q and the degree of signal superposition d_f on a given RE. Considering

single antenna UEs, MPA exhibits a complexity $\mathcal{O}(NQ^{d_f})$. Conversely, the modified EPA [31] reduces the number of messages passing by employing the QR decomposition and increases the parallelism of the algorithm. The resultant complexity exhibited from FNs to VNs reduces to $\mathcal{O}(Nd_fQ)$ while message passing from VNs to FNs reduces to $\mathcal{O}(Nd_f)$. The complexity of SIC is primarily in the computation of the decoding order metric for each user multiplexed in the layer, and is given as $\mathcal{O}(b^3)$ for a minimum mean squared error (MMSE) transformation weight matrix of $b \times b$. Consequently, the overall J-EPA-SIC receiver complexity can approximately be given by $\mathcal{O}(NQd_f + QNLb^3)$.

The complexity of the DNN is generally analysed using floating point operations (FLOPs). The DNN-SIC complexity is given as $\mathcal{O}(A_0A_1+A_1A_2+\cdots+A_mA_{M+1})$ [8] while that of a DNN-SCMA is given as $\mathcal{O}(M \cdot A_m^2)$ [20]. The fully connected DNN based MUD complexity can be approximated to $\mathcal{O}(D(A_0A_1 + M \cdot A_m^2 + A_mA_{M+1}))$. The DNN based MUD greatly reduces the exponential and multiplication terms despite having more additive terms, thereby exhibiting a reduced complexity compared to Joint EPA - SIC.

$$\mathcal{O}(NQd_f + QNLb^3) \gg \mathcal{O}(D(A_0A_1 + M \cdot A_m^2 + A_mA_{M+1})) \tag{16}$$

IV. RESULTS AND DISCUSSIONS

A. SIMULATION PARAMETERS AND SETUP

The performance evaluation and comparison of the proposed DL-MUD, SIC-MPA [3], hybrid SIC-log-MPA (HSLM) MUD that employs Log-MPA on the code-domain [5], Joint Modified SIC-EPA receiver algorithm considering single transceiver antenna [31], HMAS receiver system [26] and DNN-based receiver for PD-SCMA - visible light communication (VLC) system [28] is investigated. Resource allocation for the PD-SCMA system is performed based on the dual-parameter ranking (DPR -RA) [5]. The IFFT and CP sizes are 256 and 8 respectively. The detailed system parameters and assumptions for the uplink PD-SCMA are presented in Table 1 while the DNN model simulation parameters for the uplink PD-SCMA system are presented in Table 2.

TABLE 1. Simulation parameters.

Parameters	Symbol	Values
Minimum FU QoS	R_{min}	0.01 bps/Hz
Error variance	σ_z^2	0.01
RE Bandwidth	B_{ru}	$10MHz$
Number of FUs	K	$4-24$
Number of NUs per layer	U	$1-5$
Number of REs	N	$4-6$
signal to noise Ratio	SNR	$32dB$
Distance between NUs and BS	d_{NU}	$20-40(m)$
Distance between FUs and BS	d_{FU}	$100-150(m)$
BS peak power	P	$43dBm$

In order to evaluate the loss function performance, the batch size 32, 64, 96 and 128 on the validation set is adopted. It is observed in FIGURE 5 that the DNN converges within 300 iterations. The convergence rate reduces as the batch size enlarges. In this model, the smallest MSE for the validation set is arrived at a batch size of 64, hence its selected. Very small and very large batch sizes makes the learning process noisier and fluctuating, essentially extending the time it takes the algorithm to converge [32]. Thus it can be observed that below 64, the MSE performance reduces due to noise. Furthermore, the learning rate affects the convergence on the training and validation set. FIGURE 6 presents the system MSE system with respect to the number of iterations. A higher learning rate causes the NN to learn faster while a very small learning rate results to the NN falling into a local optimum. From FIGURE 6, beyond 300 iterations, the MSE stabilizes and when the learning rate is 0.001, the MSE becomes the smallest. The performance drops beyond this rate. These parameters are hence adopted for this DNN model application.

TABLE 2. DNN model simulation parameters.

Parameters	Values
Training data	23040
Validation data	7680
Hidden layers	6
Number of neurons in a layer	256
Activation functions	ReLU/Sigmoid
Loss functions	MSE
Batch size	64
Training / Validation Epoch	300
Learning rate	0.001
Decay rate	0.9

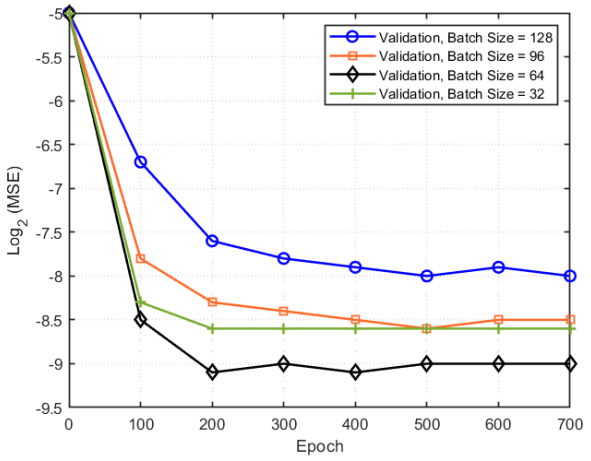

FIGURE 5. MSE versus Epoch for different validation batch sizes.

B. AVERAGE SYMBOL ERROR RATE (SER) PERFORMANCE

The average SER versus SNR for diffrent schemes considered for comparison purposes illustrated in FIGURE 7. It can be observed that the average SER for all the considered schemes decreases with increasing SNR. Besides, it is observed that the SER decreases gradually at low SNR but significantly rapidly at higher SNR values. This can be attributed to the ability of PD-SCMA system to mitigate

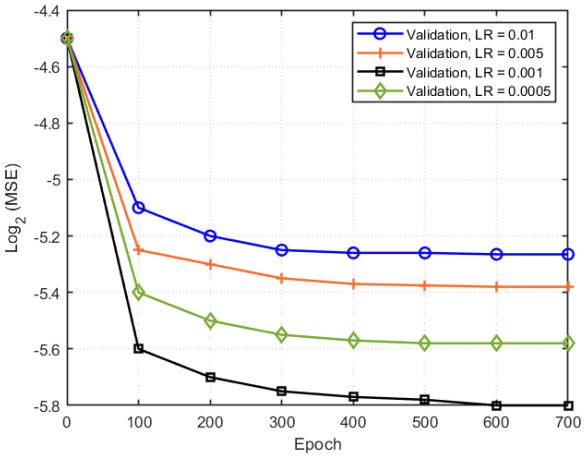

FIGURE 6. MSE versus Epoch for different learning rates.

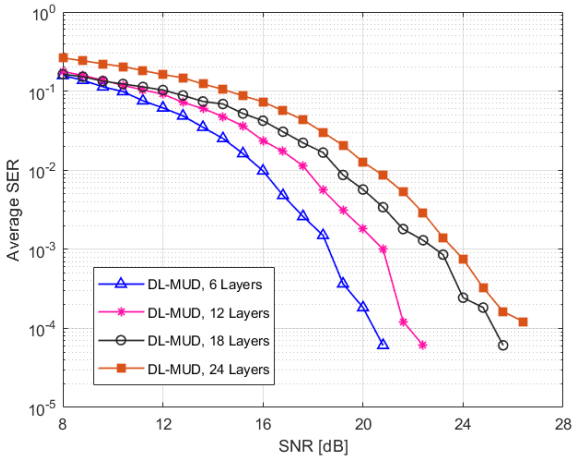

FIGURE 8. Average SER versus SNR for DL-MUD same PDMLs.

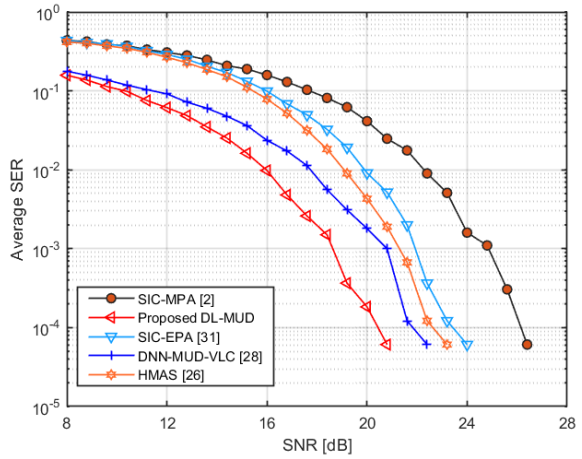

FIGURE 7. Average SER versus SNR for different PD-SCMA receiver schemes.

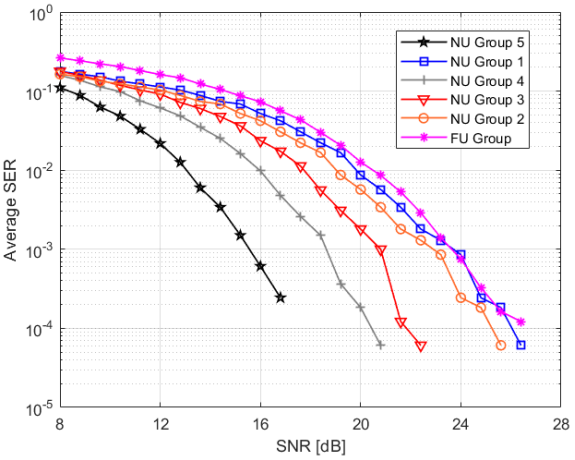

FIGURE 9. Average SER versus SNR for the different NU and FU user PDML clusters.

inter-symbol interference at high SNR. The DNN based schemes exhibit significant BER performance compared to the SIC-MPA related MUD schemes with the proposed DL-MUD outperforming the others. This is attributed to the fact that the DNN based MUD effectively learns the mapping relationship of the PD-SCMA user symbols in both code- and power-domains. Besides, the interference propagation associated with SIC-MPA detection scheme deteriorates the SER performance.

The effect of the number of layers/codebooks on the average SER as the SNR increases is illustrated in FIGURE 8. With the clustered users utilizing the same PDML, it can be observed that fewer layers result to better average SER, since the inter-symbol interference is relatively lower compared to deploying larger number of layers. The designer's choice on the number of layers is a trade-off between the overloading factor and the achievable average SER for optimal Quality of Service (QoS) requirements.

The average SER against SNR for the NU and FU user clusters/groups is illustrated in FIGURE 9. Since the FUs are allocated the highest power, by nature of SIC operation, FU group will be detected first while regarding the J NU groups as interference plus the channel noise. The FU group experiences the largest interference from all users and will exhibit lower average SER performance, while the lowest power allocated NU group effectively enjoys interference-free transmission. In this simulation, we considered $J = 5$ NU groups with $\|\mathbf{P}_1^{\mathcal{J}}\| > \|\mathbf{P}_2^{\mathcal{J}}\| > \cdots > \|\mathbf{P}_5^{\mathcal{J}}\|$. Consequently, NU group 5 will be decoded with minimal interference and hence the significant average SER performance compared to the other NU user clusters.

C. COMPUTING PERFORMANCE

FIGURE 10 presents a comparison of the execution times for different PD-SCMA detection schemes with a fixed number of NUs per codebook and fixed number of codebooks at $J = 2$ and $C = 6$ respectively. Though the computational time increases with increasing test data, the joint MPA-SIC [2], [3] exhibits the highest. The proposed DNN based detection, compared to joint log MPA-SIC [33] and joint EPA-SIC [31], exhibit greatly reduced execution times due to the reduced resource exchanges iterations

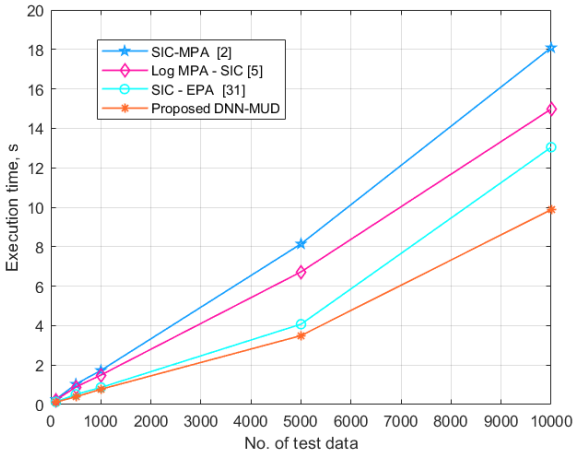

FIGURE 10. Execution time for different RA schemes.

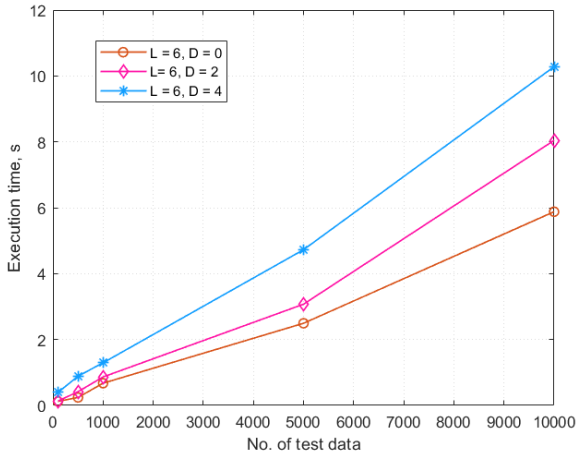

FIGURE 11. Execution time for the RA in the uplink PD-SCMA with different number of paired NUs, J.

before convergence. The proposed DNN detection that learns to approximate the proposed joint EPA-SIC has an execution time that is approx 35% lower than EPA-SIC.

FIGURE 11 shows a comparison of the execution times in a DNN based aided PD-SCMA detection with varied number of the clustered NUs, D and the number of layers fixed at $L = 6$. It is observed that as the number of clustered NUs increases, the execution time grows exponentially. Since a PD-SCMA with $D = 0$ is equivalent to a SCMA, then the execution time is lower as the elements of user clustering is eliminated. Besides, additive layer, user clustering and the resulting interference computations drastically increases the execution time.

V. CONCLUSION

A Deep Learning based multi-user detection scheme named DL-MUD is proposed in this work for an uplink PD-SCMA system consisting of NUs and FUs. The fully connected DL-MUD structure utilizes batch normalization to cancel the internal covariate shifts thus reducing the effects of overfitting. Consequently, the DNN structure improves the efficiency and reliability of neural network model to perform detection of the power distinctive NU and FU groups. Simulation results exhibit the significant advantage of the proposed DL-MUD scheme in terms of the average SER performance compared to the conventional SIC-MPA based detection schemes, due to its because of high accuracy learning of the mapping relationship of the PD-SCMA signal in both power and code domains. Besides, the proposed DL-MUD is shown to greatly perform better at high SNR values compared to low SNR values. Further work is recommended to enhance spectral efficiency and explore other machine learning based MUDs for multi-antenna hybrid NOMA techniques to enhance achievable SER.

ACKNOWLEDGMENT

The authors would like to thank Centre for Radio Access and Rural Technologies (CRART), University of KwaZulu-Natal (UKZN), for supporting this work.

REFERENCES

[1] Z. Ding, X. Lei, G. K. Karagiannidis, R. Schober, J. Yuan, and V. K. Bhargava, "A survey on non-orthogonal multiple access for 5G networks: Research challenges and future trends," *IEEE J. Sel. Areas Commun.*, vol. 35, no. 10, pp. 2181–2195, Oct. 2017.

[2] M. Moltafet, N. Mokari, M. R. Javan, H. Saeedi, and H. Pishro-Nik, "A new multiple access technique for 5G: Power domain sparse code multiple access (PSMA)," *IEEE Access*, vol. 6, pp. 747–759, 2018.

[3] S. Chege and T. Walingo, "Energy efficient resource allocation for uplink hybrid power domain sparse code nonorthogonal multiple access heterogeneous networks with statistical channel estimation," *Trans. Emerg. Telecommun. Technol.*, vol. 32, no. 1, p. e4185, Jan. 2021.

[4] S. Sharma, K. Deka, V. Bhatia, and A. Gupta, "Joint power-domain and SCMA-based NOMA system for downlink in 5G and beyond," *IEEE Commun. Lett.*, vol. 23, no. 6, pp. 971–974, Jun. 2019.

[5] S. Chege and T. Walingo, "Multiplexing capacity of hybrid PD-SCMA heterogeneous networks," *IEEE Trans. Veh. Technol.*, vol. 71, no. 6, pp. 6424–6438, Jun. 2022.

[6] Q. Luo, P. Gao, Z. Liu, L. Xiao, Z. Mheich, P. Xiao, and A. Maaref, "An error rate comparison of power domain non-orthogonal multiple access and sparse code multiple access," *IEEE Open J. Commun. Soc.*, vol. 2, pp. 500–511, 2021.

[7] M. H. Rahman, M. A. S. Sejan, M. A. Aziz, Y.-H. You, and H.-K. Song, "HyDNN: A hybrid deep learning framework based multiuser uplink channel estimation and signal detection for NOMA-OFDM system," *IEEE Access*, vol. 11, pp. 66742–66755, 2023.

[8] J. Fu, Y. Xiao, H. Liu, P. Yang, and B. Zhang, "A novel intelligent SIC detector for NOMA systems based on deep learning," in *Proc. IEEE 93rd Veh. Technol. Conf. (VTC-Spring)*, Apr. 2021, pp. 1–6.

[9] I. Sim, Y. G. Sun, D. Lee, S. H. Kim, J. Lee, J.-H. Kim, Y. Shin, and J. Y. Kim, "Deep learning based successive interference cancellation scheme in nonorthogonal multiple access downlink network," *Energies*, vol. 13, no. 23, p. 6237, Nov. 2020.

[10] J.-M. Kang, I.-M. Kim, and C.-J. Chun, "Deep learning-based MIMO-NOMA with imperfect SIC decoding," *IEEE Syst. J.*, vol. 14, no. 3, pp. 3414–3417, Sep. 2020.

[11] M. A. Aref and S. K. Jayaweera, "Deep learning-aided successive interference cancellation for MIMO-NOMA," in *Proc. IEEE Global Commun. Conf.*, Dec. 2020, pp. 1–5.

[12] J. Pan, N. Ye, A. Wang, and X. Li, "A deep learning-aided detection method for FTN-based NOMA," *Wireless Commun. Mobile Comput.*, vol. 2020, pp. 1–11, Jan. 2020.

[13] B. Brik, K. Boutiba, and A. Ksentini, "Deep learning for B5G open radio access network: Evolution, survey, case studies, and challenges," *IEEE Open J. Commun. Soc.*, vol. 3, pp. 228–250, 2022.

[14] S.-M. Tseng and W.-Y. Chen, "Cross-layer codebook allocation for uplink SCMA and PDNOMA-SCMA video transmission systems and a deep learning-based approach," *IEEE Syst. J.*, vol. 17, no. 1, pp. 294–305, Mar. 2023.
[15] W. Yu, F. Sohrabi, and T. Jiang, "Role of deep learning in wireless communications," *IEEE BITS Inf. Theory Mag.*, vol. 2, no. 2, pp. 56–72, Nov. 2022.
[16] M. Rebhi, K. Hassan, K. Raoof, and P. Chargé, "Sparse code multiple access: Potentials and challenges," *IEEE Open J. Commun. Soc.*, vol. 2, pp. 1205–1238, 2021.
[17] C. Lu, W. Xu, H. Shen, H. Zhang, and X. You, "An enhanced SCMA detector enabled by deep neural network," in *Proc. IEEE/CIC Int. Conf. Commun. China (ICCC)*, Aug. 2018, pp. 835–839.
[18] M. Kim, N.-I. Kim, W. Lee, and D.-H. Cho, "Deep learning-aided SCMA," *IEEE Commun. Lett.*, vol. 22, no. 4, pp. 720–723, Apr. 2018.
[19] X. Glorot and Y. Bengio, "Understanding the difficulty of training deep feedforward neural networks," in *Proc. 13th Int. Conf. Artif. Intell. Statist.*, 2010, pp. 249–256.
[20] J. Lin, S. Feng, Y. Zhang, Z. Yang, and Y. Zhang, "A novel deep neural network based approach for sparse code multiple access," *Neurocomputing*, vol. 382, pp. 52–63, Mar. 2020.
[21] C.-P. Wei, H. Yang, C.-P. Li, and Y.-M. Chen, "SCMA decoding via deep learning," *IEEE Wireless Commun. Lett.*, vol. 10, no. 4, pp. 878–881, Apr. 2021.
[22] M. Rebhi, K. Hassan, K. Raoof, and P. Chargé, "Deep learning for a fair distance-based SCMA detector," in *Proc. IEEE Wireless Commun. Netw. Conf. (WCNC)*, Apr. 2022, pp. 650–655.
[23] N. I. Kim and D.-H. Cho, "Hybrid multiple access system based on non orthogonality and sparse code," in *Proc. IEEE Wireless Commun. Netw. Conf. (WCNC)*, Mar. 2017, pp. 1–6.
[24] T. Sefako and T. Walingo, "Biological resource allocation algorithms for heterogeneous uplink PD-SCMA NOMA networks," *IEEE Access*, vol. 8, pp. 194950–194963, 2020.
[25] S. A. H. Mohsan, Y. Li, A. V. Shvetsov, J. Varela-Aldás, S. M. Mostafa, and A. Elfikky, "A survey of deep learning based NOMA: State of the art, key aspects, open challenges and future trends," *Sensors*, vol. 23, no. 6, p. 2946, Mar. 2023.
[26] S. Sharma and Y. Hong, "A hybrid multiple access scheme via deep learning-based detection," *IEEE Syst. J.*, vol. 15, no. 1, pp. 981–984, Mar. 2021.
[27] K. Deka and S. Sharma, "Hybrid NOMA for future radio access: Design, potentials and limitations," *Wireless Pers. Commun.*, vol. 123, no. 4, pp. 3755–3770, Apr. 2022.
[28] B. Lin, Q. Lai, J. Luo, L. Dai, N. Jiang, and T. Huang, "A deep neural networks based demodulator for PD-SCMA-VLC," *Opt. Commun.*, vol. 532, Apr. 2023, Art. no. 129256.
[29] M. Moltafet, N. M. Yamchi, M. R. Javan, and P. Azmi, "Comparison study between PD-NOMA and SCMA," *IEEE Trans. Veh. Technol.*, vol. 67, no. 2, pp. 1830–1834, Feb. 2018.
[30] H. Cheng, Y. Xia, Y. Huang, Z. Lu, and L. Yang, "Deep neural network aided low-complexity MPA receivers for uplink SCMA systems," *IEEE Trans. Veh. Technol.*, vol. 70, no. 9, pp. 9050–9062, Sep. 2021.
[31] S. Chege and T. Walingo, "MIMO hybrid PD-SCMA NOMA uplink transceiver system," *IEEE Access*, vol. 10, pp. 88138–88151, 2022.
[32] N. Yang, H. Zhang, K. Long, H.-Y. Hsieh, and J. Liu, "Deep neural network for resource management in NOMA networks," *IEEE Trans. Veh. Technol.*, vol. 69, no. 1, pp. 876–886, Jan. 2020.
[33] W. B. Ameur, P. Mary, M. Dumay, J.-F. Hélard, and J. Schwoerer, "Performance study of MPA, log-MPA and MAX-Log-MPA for an uplink SCMA scenario," in *Proc. 26th Int. Conf. Telecommun. (ICT)*, Apr. 2019, pp. 411–416.

SIMON CHEGE (Member, IEEE) received the B.Sc. degree in electrical and communications engineering from Moi University, Kenya, the M.Sc. degree in electrical and electronic engineering from JNTU Anantapur, India, and the Ph.D. degree in electronic engineering from the University of KwaZulu-Natal, Durban, South Africa. He is currently a Lecturer with the Department of Electrical and Communication Engineering, Moi University. He is also a Postdoctoral Researcher with the University of KwaZulu-Natal. He has published and reviewed papers in peer-reviewed journals. His research interests include wireless communications, multi-radio access technologies, wireless sensor networks, machine learning, and smart cities. He is a TPC member of WIDECOM and IEEE AFRICON conferences.

TOM WALINGO (Member, IEEE) received the B.Sc. degree in electrical and communications engineering from Moi University, Kenya, the M.Sc. degree in electronic engineering from the University of Natal, and the Ph.D. degree in electronic engineering from the University of KwaZulu-Natal, Durban, South Africa. He is currently a Researcher with the Center of Radio Access and Rural Technology and a Professor in communications and computer engineering with the University of KwaZulu-Natal. He has authored many peer-reviewed journals and conference papers. His current research interests include digital and wireless communications, satellite communications, and wireless sensor networks. He was a recipient of several research awards, including the SAIEE ARJ 2013 Award. He is an editor/reviewer of several journals in his field.